Published in final edited form as:
Neurotoxicology. 2012 March ; 33(2): 162–168. doi:10.1016/j.neuro.2012.01.001.

Microarray genomic profile of mitochondrial and oxidant response in Manganese Chloride treated PC12 cells

Equar Taka[a], **Elizabeth Mazzio**[a], **Karam FA Soliman**[a], and **R. Renee Reams**[a,*]
[a]College of Pharmacy and Pharmaceutical Sciences, Florida A & M University, Tallahassee, Florida 32307, USA.

Abstract

Environmental or occupational exposure to high levels of manganese (Mn) can lead to manganism, a symptomatic neuro-degenerative disorder similar to idiopathic Parkinson's disease. The underlying mechanism of Mn neurotoxicity remains unclear. In this study, we evaluate the primary toxicological events associated with $MnCl_2$ toxicity in rat PC12 cells using whole genome cDNA microarray, RT-PCR, western blot and functional studies. The results show that a sub-lethal dose range (38–300 μM $MnCl_2$) initiated slight metabolic stress evidenced by heightened glycolytic rate and induction of enolase / aldolase - gene expression. The largest shift observed in the transcriptome was $MnCl_2$ induction of heme-oxygenase 1 (HO-1) [7.7 fold, $p < 0.001$], which was further corroborated by RT-PCR and western blot studies. Concentrations in excess of 300 μM corresponded to dose dependent loss of cell viability which was associated with enhanced production of H_2O_2 concomitant to elevation of of gene expression for diverse antioxidant enzymes; biliverdin reductase, arsenite inducible RNA associated protein, dithiolethione-inducible gene-1 (DIG-1) and .thioredoxin reductase 1. Moreover, Mn initiated significant reduction of gene expression of mitochondrial glutaryl-coenzyme A dehydrogenase (GCDH) -, an enzyme involved with glutaric acidemia, oxidative stress, lipid peroxidation and striatal degeneration observed in association with severe dystonic dyskinetic movement disorder. Future research will be required to elucidate a defined role for HO-1 and GCDH in Mn toxicity.

Keywords

manganese; dopamine; heme oxygenase; mitochondria; cDNA microarray whole genome; GCDH

1. Introduction

Manganese is an essential trace metal required for proper immune function, metabolism, reproduction, digestion, bone growth, and blood clotting (dos Santos et al., 2010). Additionally, Mn functions as a cofactor in several enzymes such as arginase (urea formation), glutamine synthetase (for brain ammonia metabolism), Mn superoxide dismutase (MnSOD) (antioxidant) and phosphoenolpyruvate decarboxylase

*Corresponding Author Romonia Renee Reams, Ph.D, College of Pharmacy & Pharmaceutical Sciences, Florida A&M University, Room 126 Dyson Pharmacy Building, 1520 ML King Blvd, Tallahassee, FL 32307, Phone 850 561-2672 or FAX 850 599-3171, renee.reams@famu.edu.

Conflict of Interest statement
There are no conflict of interests to declare.

(gluconeogenesis) (Christianson, 1997, Paynter, 1980). While dietary intake of Mn is essential to prevent deficiencies, exposure to high levels of Mn can be toxic leading to irreversible neurological injury (Greger, 1999).

Chronic exposure to higher levels of Mn in occupational and environmental settings can arise in association with steel production, gasoline anti-knock additives (methylcyclopentadienyl manganese tricarbonyl), mining, welding, battery assembly and glass and ceramics manufacturing (Aschner et al. , 2005). It is estimated that over 3700 tons of Mn are released into the atmosphere every year (Sengupta et al. , 2007). High level exposure can lead to manganism which is a progressive disease with symptoms similar to those of Parkinson's disease (Lucchini et al. , 1999). Typical symptoms include tiredness, sleep disturbances, aggressiveness, and behavioral disturbances ("manganese madness"). Delayed neurological disturbances encompass the extrapyramidal system, characterized by walking difficulties, dystonia, and kinesia (dos Santos, Milatovic, 2010). The similarities between symptomic cardinal signs associated with acute Mn toxicity in humans and idiopathic PD are indicative of deficiency of dopamine in the striatum. In PD a loss of dopamergic neurons in the SNc occurs in addition to progressive losses of the dopamine transporter and dopa decarboxylase, where Mn accumulates in the basal ganglia, damages the D2 receptor, inhibits the dopamine transporter and results in toxicological insult to the globus pallidus (Ericson et al. , 2007, Guilarte, 2011, Winder et al. , 2010). While both result in dopamine deficiency and are responsive to L-dopa therapy, there seems to be differences in regional patterned damage associated with Mn toxicity and PD. Moreover, the leading mechanism of manganese neurotoxicity is not clear, however, several studies have suggested that Mn induces neuronal cell death by disrupting mitochondrial function (Malecki, 2001), initiating oxidative stress (Chtourou et al. , 2010), altering MAPK signaling, disrupting cellular calcium and iron homeostasis (Reaney and Smith, 2005) an initiating cytochrome c release and apoptosis (Roth et al. , 2002).

Genomic microarrays are a valuable tool in probing or identifying molecular patterns associated with environmental exposure to diverse toxins. In this study, we employ this technique to elucidate the nature of changes incurred when treating PC12 cells (which synthesize/ release catecholamines) with varying concentrations of Mn. The findings while broad, provide general identification of major genes or protein shifts incurred by Mn, which were corroborated by RT-PCR and immuno-blotting.

2.Materials and methods

2.1 Chemicals and Materials

Pheochromocytoma (PC12) cells (ATCC, Manassas, VA), RPMI Media 1640, horse serum (HS), fetal bovine serum (FBS), and penicillin/streptomycin, trypan blue exclusion, tissue culture water , MnCl2, Chloroform, Isopropyl alcohol, 10X PBS, Tween twenty, (Sigma Chemical Company, St. Louis, MO); TrizolTMLS reagent (Gibco BRL, NY, USA); Nuclease-free water (Ambion the RNA Company, Austin, TX); MultiScribe™ Reverse Transcriptase (RT), 10X RT buffer, 10X random primers, 25X dNTPs, 2X Master Mix, Probe/gene set (Assay)(Applied Biosystem, Foster City, CA); Agilent Rat cDNA Microarray from Incyte Genomics and cDNA synthesis kit (Agilent Technologies Inc, CA),

2.2 Cell Cultures and Trypan Blue Cell Viability

PC12 cells are derived from rat adrenal medulla pheochromocytoma of dopaminergic origin, often used as a model to study various aspects of catecholaminergic function. PC12 cells were cultured in RPMI media supplemented with 10% HS, 5% FBS, 25 units/ml penicillin, and 25 μg/ml streptomycin. These cells were grown at 37°C in a humidified atmosphere of

5% CO_2 incubator. The culture media was changed every 2–3 days until the cells reached confluence. Viability of PC12 cells were assessed using Trypan Blue Exclusion. Only cells with viability greater or equal to 90% were used to set an experiments.

2.3 RNA Extraction and Agilent Rat cDNA Microarray Analysis

To examine the effect of Mn on PC12 cells gene expression two groups of samples were prepared as follows: (1) untreated PC12 cells, which served as controls and (2) 300μM $MnCl_2$ treated PC12 cells. For each group, approximately 1×10^7 cells were plated in duplicate in 75cm flask and incubated overnight at 37°C to attach. The next day cells were treated with 300μM $MnCl_2$ and incubated again for 24 hrs. At the end of 24hr exposure to $MnCl_2$ total RNA was isolated using TrizolTM LS reagent following the manufacturer protocol (Gibco BRL, NY). The integrity of the total RNA isolated was monitored using an Agilent 2100 Bioanalyzer System; all samples exhibit a ratio of 1.9–2.1. Agilent Rat cDNA microarray experiment analysis was performed at Wayne State University. The microarray contained approximately 10,900 sequence- verified cDNAs from Incyte Genomic.

2.4 Microarray Data Analysis and Statistics

Microarray data were analyzed GeneSifter software (GeneSifter is now Geospiza, Seattle, WA.). To identify genes whose transcript level was significantly altered by Mn, we applied three consecutive analysis processes. First, we applied pairwise analysis to identify genes whose overall transcript level calculated from three independent experiment (Mn-treated versus control) was altered by at least 1.5-fold. Second, Gene Ontology and z-score repot were also generated with GeneSifter. Statistical analysis of individual gene expression data was performed with Student's t-test. (http://genesifter.net/datacenter/).

2.5 Validation of Heme Oxygenase cDNA results by RT-PCR

The technique RT-PCR was used to confirm the results from the cDNA microarray study, for heme oxygenase 1 (HO-1). The primers used were as follows: Heme oxygenase 1, - product size 376bp, forward, 5'-TTC ACC TTC CCG AGC ATC-3' reverse 5'-TCC CAC TGC CAC GGT C-3'; For normalization 40S ribosomal protein S29 (RPS29) housekeeping gene was used. The primer used was, product size 276bp, forward, 5'-CTC CTT GGG CGT CTG A-3' reverse 5'-GCG CAA AGA CTA GCA TGA-3'. The RTPCR program included first reverse transcription (RT) of RNA by StrataScriptTM reverse transcriptase (StrataScriptTM RT) at 42°C for 15 minutes then PCR program follows. The amplification program included the initial denaturation step at 95°C for 1 minute and - 30 cycles of denaturation at 95°C for 30s, annealing at (66°C for - HO-1 and 63°C RPS29) for 30s, and extension at − 68°c for 2 minutes and 10 minute final extension at 68°C. Aliquots of the PCR products (20 μL) were visualized with ethidium bromide staining after separation by electrophoresis in a 2% agarose gel in Tris borate ethylenediamine tetra-acetic acid buffer pH 8.3 at 100V for 2 h. Images were captured by a Fluor-S Max MultiImaging system and *Band intensities were measured using Molecular Dynamics 300 Series Computing Densitometer*.

2.6 Western blotting analysis

Expression of protein level of HO-1 was assessed by Western blot analysis in PC12 cell lysates. Total protein (20μg) was derived from cell lysates of PC12 cells treated with 38μM, 75μM, 150 μM, 300 μM, 600 μM, 1200 μM $MnCl_2$ and control PC12 cells (no treatment) were subjected to SDS-polyacrylaminde gel electrophoresis (PAGE) on 10% polyacrylamide gel, then transferred to a nitrocellulose membrane. Blots were probed with anti-heme oxygenase 1 (Santa Cruz Biotechnology, Santa Cruz, CA) overnight 4°C at a concentration 1:800 in 5% milk/PBS with 0.05% Tween-20. The membrane was then

incubated with anti-rat IgG horseradish peroxide-linked secondary antibody (Santa Cruz Biotechnology, Santa Cruz, CA) at a concentration of 1:1000 for three hours at room temperature. Blots were then rinsed thoroughly in PBS with tween-20 (PBS-T), and visualized with chemiluminescence. The nitrocellulose membrane was then stripped at 50°C for 30 minutes in stripping solution (2% SDS, 0.1M β-mercaptoethanol, and 0.06M TRIS, PH 6.8), then was rinsed twice for 10 minutes with PBS with tween-20. The blots were probed with anti-beta actin (Santa Cruz Biotechnology, Santa Cruz, CA) at a concentration 1:600 in 5% milk/PBS with tween-20 overnight at 4°C. This was followed by 3 hour incubation with the secondary antibody anti-rat IgG (Santa Cruz Biotechnology, Santa Cruz, CA) at a concentration of 1:1000 in 5% milk/PBS with tween-20. Blots were then rinsed with PBS visualized by chemiluminescence and exposed to radiographic film (Kodak X-OMAT AR). Film images were scanned and protein band intensities were quantitated using *Molecular Dynamics 300 Series Computing Densitometer*.

2.7 Cell metabolism

Cell viability was assessed using resazurin (Alamar Blue) indicator dye (Evans et al. , 2001). A working solution of *resazurin* was prepared in sterile PBS - phenol red (0.5 mg/ml) and added (15% v/v) to each sample. Samples were returned to the incubator for 6–8 hr, and reduction of the dye by viable cells (to *resorufin*, a fluorescent compound) was quantitatively analyzed on a microplate fluorometer, Model 7620, version 5.02 (Cambridge Technologies Inc, Watertown, MA) with settings at [550/580], [excitation/emission].

2.8 HPLC Quantification of Lactic Acid and Glucose

Lactate and glucose concentrations were determined using a Shimadzu HPLC system equipped with an SPD-*20A* UV detector (set at 210 *nm*), a RID-*10A* 120V refractive index detector, a workstation containing EZSTART V7.4 software and an SS420X instrument interface docked to a Waters Autosampler Model 717 Plus (Shimadzu Scientific Instruments, Inc. US; Waters Corp., Milford, MA). The flow rate was isocratic controlled by a Waters Model 510 pump and set at 0.6 ml/min. The mobile phase consisted of 5 mM sulfuric acid, the column was an aminex HPX-87H 300 × 7.8 mm, carbohydrate analysis column, 9 μm particle size (Biorad Hercules, CA), run time was 16 min and injection volume 25 μl. Samples were prepared by placing 35 μl cell supernatant directly into 200ul of 5mM sulfuric acid, immediately stored at –80C. Prior to analysis, samples were thawed and 125 μl, mixed with 275 μl of the 5mM sulfuric acid, vortexed, capped and analyzed. Glucose and lactate standard curves were prepared in distilled water and matrix blank controls and spikes were run for every experimental treatment condition tested.

2.9 Hydrogen Peroxide Measurement

Hydrogen peroxide was assessed using a chromogenic solution containing 1 mM vanillic acid, 500μM of 4-aminoantipyrine and 4 U/ml purpurogallin of horse-radish peroxidase—type II (Mazzio and Soliman, 2004). The combined reagent was added to each sample and returned to the incubator, continuous endpoint analysis was monitored at 500 nm using a UV microplate spectrophotometer, Model 7600 version 5.02, Cambridge Technologies Inc. (Watertown, MA, USA).

3. Results

PC12 cells were exposed to $MnCl_2$ over a concentration range of 38– 4800 μM for 24 hrs (Figure 1). The dose dependent toxicological profile shows a sub-lethal range (38–300 μM) with greater concentrations associated with cell death. In order to evaluate metabolic changes altered by $MnCl_2$, lactate and glucose concentrations in the media were evaluated by HPLC at 24 hr (Figure 2). The data show a very slight shift toward enhanced glycolytic

activity as evidenced by rise in lactate and expedited utilization of glucose from 38–300μM, with losses that paralleled toxicity at higher concentration. However, these changes are very mild in comparison to that observed with various mitochondrial toxins such as MPP+ (Mazzio and Soliman, 2003) which evoke cell death by loss of cellular respiration, accelerated glycolysis and ultimately exhaustion of glucose supplies. In this study, losses of glucose were meager and ample quantities of glucose remained in the media at 300μM $MnCl_2$ to sustain energy metabolism, indicating that energy failure is not the primary cause of cell death.

In order to determine if production of H_20_2 and superoxide corresponded to $MnCl_2$ induced cell death, free radicals were quantified. The data show that only H_20_2 was detected after 24 Hrs, while we found no evidence for rise in superoxide using cytochrome c reduction methods (data not shown) (Figure 3). These findings show an inverse linear relationship between cell death and production of H_20_2 suggesting that oxidative stress may be involved with toxicity.

In order to gain understanding as to the molecular changes incurred by $MnCl_2$, cDNA microarray analysis was conducted. The data in Figs 1–3 establish 300μM to be an appropriate concentration to capture molecular events associated with $MnCl_2$ at concentrations just below the threshold of toxicity (< 600μM Mn). Therefore, whole genome microarray analysis was performed by comparing untreated controls vs PC12 cells exposed to 300μM $MnCl_2$. The data show that Mn significantly ($p < 0.05$) altered the expression of 223 genes (out of 10,900 genes) whose overall expression level was >1.5- fold. Of these 223 genes, 146 were up-regulated while 77 were down-regulated. Sixty nine of these genes were expressed at more than two folds, and an additional 16 genes were expressed at greater than three fold with the highest for heme oxygenase 1 (H0-1) (7.70-fold increase). Genes which displayed differential patterns ($p<.05$) involved in either metabolism or antioxidant response are presented in Table 1. HO-1 has the highest gene expression (7.70-fold increase).

In order to further corroborate the effects of $MnCl_2$ on HO-1, RT-PCR was performed (Figure 4A, 4B), followed by protein expression analysis using SDS-PAGE/Western blot (Figure 5 A–C). Both RT-PCR and western blot findings are consistent with gene expression profile showing greatest HO-1 expression at 300μM $MnCl_2$, non – existent in controls, where induction occurred at 12h but reached a maximum value at 18–24 hrs. The results from these studies suggest that HO-1 plays a predominant role, albeit not well understood, in molecular effects of $MnCl_2$ in PC12 cells.

4. Discussion

The purpose of the present study was to evaluate the primary toxicological events associated with Mn toxicity in rat PC12 cells using cDNA microarray, RT-PCR, western blot and functional studies. These findings show that Mn toxicity is primarily associated with induction of heme oxygenase 1 , elevated production of H_20_2, with very slight effects on loss of mitochondria with exception for loss of mitochondrial glutaryl-CoA dehydrogenase (GCDH), reduction which is typically associated with striatal lesions specific to the basal ganglia (Strauss et al. , 2007). The findings in this study corroborate a number of previous studies having demonstrated that toxicity of Mn is associated with induction of HO-1 (Satarug et al. , 2008) and greater oxidative stress as evidenced by lipid peroxidation, reduction of endogenous antioxidants system (SOD, CAT, GPx) and depletion of antioxidants (GSH, Vit C) (Chtourou, Fetoui, 2010). However, the data do not provide evidence to support Mn induced production of superoxide, or expression of MnSOD, although these effects have been reported in other models (Chiu et al. , 2002, Hussain and Ali, 1999, Methy et al. , 2004).

The largest shift in the genome was Mn induced up-regulation of HO-1. It is believed that HO-1 can serve as an antioxidant due to its ability to degrade the oxidant heme. Unbound heme is associated with the pathology of oxidative stress disorders, where a rise in HO-1 results in its removal with subsequent conversion to carbon monoxide (CO), ferrous iron (Fe2+) and biliverdin. In turn, biliverdin is converted to bilirubin (antioxidant) by biliverdin reductase (Pae and Chung, 2009). HO-1 is also considered an anti-inflammatory due to its down-regulation of cyclooxygenase-2 and a number of pro-inflammatory cytokines (tumor necrosis factor-α, interleukins 1–6) (Vijayan et al. , 2010).

The signaling pathways which control induction of HO-1 are largely mediated by the antioxidant response element (ARE) pathway controlled by nuclear localization and binding of nuclear factor-erythroid 2-related factor 2 (Nrf2) transcription factor, both co-expressed in various biological tissue, showing potent downregulators of ROS and lipid peroxidative damage (Li et al. , 2011c). A loss of the ARE antioxidant pathway, for example in Nrf2(−/−) mice establishes greater vulnerability to a number of degenerative pathologies (Zhao et al. , 2011). Li et al. have shown that in PC12 cells, the effects of Mn on induction of HO-1 are in fact mediated through Nrf2-ARE pathway (Li et al. , 2011b). Nrf2 is multifunctional, and can also up-regulate a host of related protective elements such as phase II detoxification enzymes, glutathione peroxidase (GPX) , γ-GCS (Li et al. , 2011a) and biosynthesis of intracellular glutathione (Collinson et al. , 2011, Escartin et al. , 2011). Moreover, additional down stream effects of the Nrf2-ARE include the Kelch-like ECH-associated protein 1, NADPH: quinone oxidoreductase 1, activating transcription factor 3, peroxiredoxins 3/6 and catalase (Maruyama et al. , 2011). In general, previous reports are consistent in demonstrating that Nrf2 controls HO-1 induction (Zhang et al. , 2007) , antioxidant systems through Akt, extra-cellular signal-regulated protein kinase1/2 (ERK1/2) and p38-MAPK (Na et al. , 2008). (Izumi et al. , 2011, Jiang and Dai, 2011, Mizuno et al. , 2011). Further it has been reported that Nrf-2 induction HO-1 is regulated by ERK (Chin et al. , 2011).

The findings in the current study bring forth a number of questions regarding a role for HO-1 during Mn exposure. First, - what is the origin of peroxide, does it occur through Mn - autoxidation of dopamine or another biological means. Second, since HO enzymes (HO-1 and HO-2) degrade heme into biliverdin, carbon monoxide and iron (Motterlini et al. , 2005, Wang, 2010), CO in turn could be a component to the moderate loss of mitochondrial respiratory function as observed in this study. The data in this study, show a very mild shift toward anaerobic systems in the presence of Mn that are atypical to mitochondrial toxins such as MPP+ (Mazzio and Soliman, 2003). The toxicological profile of a mitochondrial toxin is associated with extremely high levels of lactic acid, that correspond to inverse exhaustion of glucose supply – where cell starvation is the cause of cell death. In this study, toxicity occurs at a dose of Mn where abundant glucose is still present, but where high concentrations of H_20_2 predominate. The potentiating effects of Mn on HO-1 could also generate free ferrous iron, which could interact with H_20_2 in fenton reactions to generate toxic hydroxyl radicals (Whittle and Varga, 2010). For these reasons, it remains unclear as to if HO-1 is detrimental or protective.

In this study, differential expression in the genome show an up-regulation of additional antioxidant related proteins. For example Mn induction of dithiolethione-inducible gene-1 (DIG-1). DIG-1 is a component of detoxification through NAD(P)H-dependent alkenal /one oxidoreductase which can also attenuate lipid peroxidation by antagonizing products such as 4-hydroxy-2-nonenal and acrolein (Dick et al. , 2001). The sequence of DIG-1 is similar to leukotriene B4 (LTB4) B12-hydroxydehydrogenase, which can convert LTB4 to 12-oxo-LTB4 and remove free radicals (Primiano et al. , 1998).. There was also an upregulation of genes protecting against metal toxicity such as the case of arsenite inducible RNA associated protein (Airap). Airap is associated with higher expression levels of HO-1, γ-

glutamylcysteine and metallothioneins a part of a metal/ROS detoxification system which involves NFκB or eIF2α signaling, and expression of CHOP/GADD153 genes (Sok et al. , 2001) Future research will be required to assess if Mn induction of HOX-1 in PC-12 cells involves these pathways.

Genomic analysis provided evidence for several points of mitochondrial transcription repression. A large fold change was observed for mitochondrial glutaryl-coenzyme A (CoA) dehydrogenase (GCDH). GCCH is involved with decarboxylation reactions yielding products such as crotonyl-CoA, or dehydrogenation without release of CO_2 forming glutaconyl-CoA (Schaarschmidt et al. , 2011). The function of this protein is not well known, however autosomal recessive disorders which involve a mutation or loss of function, correlated to glutaric aciduria type 1 (GA1). GA1 is associated with accumulation of dicarboxylates glutaric acid and 3-hydroxyglutaric acid , largely in the brain which could adversely affect succinate transport systems and striatal complex II function (Bjugstad et al. , 2006, Lamp et al. , 2011) In this study, we also saw adverse effects specific to genome for transcription of complex II. One of the main symptoms of GA1 or GCDH deficiency is a sudden onset of dystonia which results from striatal lesions concurrent to damage to the basal ganglia, (Strauss, Lazovic, 2007). Accumulation of glutaric acid causes neurotoxicity in the basal ganglia and fronto-temporal cortex which is associated with the progressive dystonia, hypotonia, seizures. (de Luis et al. , 2007) and motor disability associated with signal abnormalities in the putamen, caudate, pallidum and ventricles (Harting et al. , 2009). Moreover, elevation of glutaric acid and 3-hydroxyglutaric acid are associated with thiobarbituric acid-reactive substances (lipid peroxidation) in astroglioma (Quincozes-Santos et al. , 2010) and elevated levels of H_20_2 and malondialdehyde in striatal homogenates (Latini et al. , 2005), Future research will be required to evaluate if glutaric acid is associated with the elevation of H_20_2 in Mn treated PC12 cells.

In conclusion the results from this work suggest that $MnCl_2$ toxicity is associated with induction of HO-1 and elevated production of H_20_2, with very slight effects on loss of mitochondrial function. Future research will be required to determine in depth signaling systems involved with this response.

Acknowledgments

This research was supported by a *grants* from Association Of Minority Health Professions Schools, Inc (AMPHS) & the ATS/DR Cooperative Agreement Number: 3U50TS473408-05W1/CFDA Number 93.161 (RRR) ; NIEHS/ ARCH 5S11ES01187-05 (RRR) ; *NIH* NCRR *RCMI* program (G12RR 03020) (KFAS)

REFERENCES

Aschner M, Erikson KM, Dorman DC. Manganese dosimetry: species differences and implications for neurotoxicity. Crit Rev Toxicol. 2005; 35:1–32. [PubMed: 15742901]

Bjugstad KB, Crnic LS, Goodman SI, Freed CR. Infant mice with glutaric acidaemia type I have increased vulnerability to 3-nitropropionic acid toxicity. J Inherit Metab Dis. 2006; 29:612–619. [PubMed: 16944278]

Chin YT, Liao YW, Fu MM, Tu HP, Shen EC, Nieh S, et al. Nrf-2 Regulates Cyclosporine-stimulated HO-1 Expression in Gingiva. J Dent Res. 2011; 90:995–1000. [PubMed: 21622902]

Chiu H, Brittingham JA, Laskin DL. Differential induction of heme oxygenase-1 in macrophages and hepatocytes during acetaminophen-induced hepatotoxicity in the rat: effects of hemin and biliverdin. Toxicol Appl Pharmacol. 2002; 181:106–115. [PubMed: 12051994]

Christianson DW. Structural chemistry and biology of manganese metalloenzymes. Prog Biophys Mol Biol. 1997; 67:217–252. [PubMed: 9446936]

Chtourou Y, Fetoui H, Sefi M, Trabelsi K, Barkallah M, Boudawara T, et al. Silymarin, a natural antioxidant, protects cerebral cortex against manganese-induced neurotoxicity in adult rats. Biometals. 2010; 23:985–996. [PubMed: 20503066]

Collinson EJ, Wimmer-Kleikamp S, Gerega SK, Yang YH, Parish CR, Dawes IW, et al. The yeast homolog of heme oxygenase-1 affords cellular antioxidant protection via the transcriptional regulation of known antioxidant genes. J Biol Chem. 2011; 286:2205–2214. [PubMed: 21081499]

de Luis E, Larrache J, Garcia-Eulate R, Garcia JN, Zubieta JL. Neuroradiologic findings of glutaric aciduria type I. Rev Med Univ Navarra. 2007; 51:9–12. [PubMed: 18183780]

Dick RA, Kwak MK, Sutter TR, Kensler TW. Antioxidative function and substrate specificity of NAD(P)H-dependent alkenal/one oxidoreductase. A new role for leukotriene B4 12-hydroxydehydrogenase/15-oxoprostaglandin 13-reductase. J Biol Chem. 2001; 276:40803–40810. [PubMed: 11524419]

dos Santos AP, Milatovic D, Au C, Yin Z, Batoreu MC, Aschner M. Rat brain endothelial cells are a target of manganese toxicity. Brain Res. 2010; 1326:152–161. [PubMed: 20170646]

Ericson JE, Crinella FM, Clarke-Stewart KA, Allhusen VD, Chan T, Robertson RT. Prenatal manganese levels linked to childhood behavioral disinhibition. Neurotoxicol Teratol. 2007; 29:181–187. [PubMed: 17079114]

Escartin C, Won SJ, Malgorn C, Auregan G, Berman AE, Chen PC, et al. Nuclear factor erythroid 2-related factor 2 facilitates neuronal glutathione synthesis by upregulating neuronal excitatory amino acid transporter 3 expression. J Neurosci. 2011; 31:7392–7401. [PubMed: 21593323]

Evans SM, Casartelli A, Herreros E, Minnick DT, Day C, George E, et al. Development of a high throughput in vitro toxicity screen predictive of high acute in vivo toxic potential. Toxicology in vitro : an international journal published in association with. BIBRA. 2001; 15:579–584.

Greger JL. Nutrition versus toxicology of manganese in humans: evaluation of potential biomarkers. Neurotoxicology. 1999; 20:205–212. [PubMed: 10385884]

Guilarte TR. Manganese and Parkinson's disease: a critical review and new findings. Ciencia & saude coletiva. 2011; 16:4519–4566.

Harting I, Neumaier-Probst E, Seitz A, Maier EM, Assmann B, Baric I, et al. Dynamic changes of striatal and extrastriatal abnormalities in glutaric aciduria type I. Brain. 2009; 132:1764–1782. [PubMed: 19433437]

Hussain S, Ali SF. Manganese scavenges superoxide and hydroxyl radicals: an in vitro study in rats. Neurosci Lett. 1999; 261:21–24. [PubMed: 10081917]

Izumi Y, Kume T, Akaike A. Regulation of dopaminergic neuronal death by endogenous dopamine and proteasome activity. Yakugaku Zasshi. 2011; 131:21–27. [PubMed: 21212609]

Jiang G, Dai AG. The pathway of PI3k/Akt-aPKCiota/zeta-Nrf2 regulating the expression of gamma-glutamylcysteine synthetase in the bronchial epithelial cells of rats. Zhongguo Ying Yong Sheng Li Xue Za Zhi. 2011; 27:115–119. [PubMed: 21560358]

Lamp J, Keyser B, Koeller DM, Ullrich K, Braulke T, Muhlhausen C. Glutaric aciduria type 1 metabolites impair the succinate transport from astrocytic to neuronal cells. J Biol Chem. 2011; 286:17777–17784. [PubMed: 21454630]

Latini A, Scussiato K, Leipnitz G, Dutra-Filho CS, Wajner M. Promotion of oxidative stress by 3-hydroxyglutaric acid in rat striatum. J Inherit Metab Dis. 2005; 28:57–67. [PubMed: 15702406]

Li H, Wang F, Zhang L, Cao Y, Liu W, Hao J, et al. Modulation of Nrf2 expression alters high glucose-induced oxidative stress and antioxidant gene expression in mouse mesangial cells. Cell Signal. 2011a

Li H, Wu S, Shi N, Lian S, Lin W. Nrf2/HO-1 pathway activation by manganese is associated with reactive oxygen species and ubiquitin-proteasome pathway, not MAPKs signaling. J Appl Toxicol. 2011b

Li M, Zhang X, Cui L, Yang R, Wang L, Liu L, et al. The neuroprotection of oxymatrine in cerebral ischemia/reperfusion is related to nuclear factor erythroid 2-related factor 2 (nrf2)- mediated antioxidant response: role of nrf2 and hemeoxygenase-1 expression. Biol Pharm Bull. 2011c; 34:595–601. [PubMed: 21532144]

Lucchini R, Apostoli P, Perrone C, Placidi D, Albini E, Migliorati P, et al. Long-term exposure to "low levels" of manganese oxides and neurofunctional changes in ferroalloy workers. Neurotoxicology. 1999; 20:287–297. [PubMed: 10385891]

Malecki EA. Manganese toxicity is associated with mitochondrial dysfunction and DNA fragmentation in rat primary striatal neurons. Brain Res Bull. 2001; 55:225–228. [PubMed: 11470319]

Maruyama A, Nishikawa K, Kawatani Y, Mimura J, Hosoya T, Harada N, et al. The novel Nrf2-interacting factor KAP1 regulates susceptibility to oxidative stress by promoting the Nrf2-mediated cytoprotective response. Biochem J. 2011; 436:387–397. [PubMed: 21382013]

Mazzio E, Soliman KF. D-(+)-glucose rescue against 1-methyl-4-phenylpyridinium toxicity through anaerobic glycolysis in neuroblastoma cells. Brain Res. 2003; 962:48–60. [PubMed: 12543455]

Mazzio EA, Soliman KF. Glioma cell antioxidant capacity relative to reactive oxygen species produced by dopamine. J Appl Toxicol. 2004; 24:99–106. [PubMed: 15052604]

Methy D, Bertrand N, Prigent-Tessier A, Stanimirovic D, Beley A, Marie C. Differential MnSOD and HO-1 expression in cerebral endothelial cells in response to sublethal oxidative stress. Brain Res. 2004; 1003:151–158. [PubMed: 15019574]

Mizuno K, Kume T, Muto C, Takada-Takatori Y, Izumi Y, Sugimoto H, et al. Glutathione biosynthesis via activation of the nuclear factor E2-related factor 2 (Nrf2)--antioxidantresponse element (ARE) pathway is essential for neuroprotective effects of sulforaphane and 6-(methylsulfinyl) hexyl isothiocyanate. J Pharmacol Sci. 2011; 115:320–328. [PubMed: 21358121]

Motterlini R, Mann BE, Foresti R. Therapeutic applications of carbon monoxide-releasing molecules. Expert opinion on investigational drugs. 2005; 14:1305–1318. [PubMed: 16255672]

Na HK, Kim EH, Jung JH, Lee HH, Hyun JW, Surh YJ. (-)-Epigallocatechin gallate induces Nrf2-mediated antioxidant enzyme expression via activation of PI3K and ERK in human mammary epithelial cells. Arch Biochem Biophys. 2008; 476:171–177. [PubMed: 18424257]

Pae HO, Chung HT. Heme oxygenase-1: its therapeutic roles in inflammatory diseases. Immune Netw. 2009; 9:12–19. [PubMed: 20107533]

Paynter DI. Changes in activity of the manganese superoxide dismutase enzyme in tissues of the rat with changes in dietary manganese. J Nutr. 1980; 110:437–447. [PubMed: 7359215]

Primiano T, Li Y, Kensler TW, Trush MA, Sutter TR. Identification of dithiolethione-inducible gene-1 as a leukotriene B4 12-hydroxydehydrogenase: implications for chemoprevention. Carcinogenesis. 1998; 19:999–1005. [PubMed: 9667737]

Quincozes-Santos A, Rosa RB, Leipnitz G, de Souza DF, Seminotti B, Wajner M, et al. Induction of S100B secretion in C6 astroglial cells by the major metabolites accumulating in glutaric acidemia type I. Metab Brain Dis. 2010; 25:191–198. [PubMed: 20437086]

Reaney SH, Smith DR. Manganese oxidation state mediates toxicity in PC12 cells. Toxicol Appl Pharmacol. 2005; 205:271–281. [PubMed: 15922012]

Roth JA, Horbinski C, Higgins D, Lein P, Garrick MD. Mechanisms of manganese-induced rat pheochromocytoma (PC12) cell death and cell differentiation. Neurotoxicology. 2002; 23:147–157. [PubMed: 12224755]

Satarug S, Kikuchi M, Wisedpanichkij R, Li B, Takeda K, Na-Bangchang K, et al. Prevention of cadmium accumulation in retinal pigment epithelium with manganese and zinc. Exp Eye Res. 2008; 87:587–593. [PubMed: 18948096]

Schaarschmidt J, Wischgoll S, Hofmann HJ, Boll M. Conversion of a decarboxylating to a non-decarboxylating glutaryl-coenzyme A dehydrogenase by site-directed mutagenesis. FEBS Lett. 2011; 585:1317–1321. [PubMed: 21477586]

Sengupta A, Mense SM, Lan C, Zhou M, Mauro RE, Kellerman L, et al. Gene expression profiling of human primary astrocytes exposed to manganese chloride indicates selective effects on several functions of the cells. Neurotoxicology. 2007; 28:478–489. [PubMed: 17175027]

Sok J, Calfon M, Lu J, Lichtlen P, Clark SG, Ron D. Arsenite-inducible RNA-associated protein (AIRAP) protects cells from arsenite toxicity. Cell Stress Chaperones. 2001; 6:6–15. [PubMed: 11525245]

Strauss KA, Lazovic J, Wintermark M, Morton DH. Multimodal imaging of striatal degeneration in Amish patients with glutaryl-CoA dehydrogenase deficiency. Brain. 2007; 130:1905–1920. [PubMed: 17478444]

Vijayan V, Mueller S, Baumgart-Vogt E, Immenschuh S. Heme oxygenase-1 as a therapeutic target in inflammatory disorders of the gastrointestinal tract. World J Gastroenterol. 2010; 16:3112–3119. [PubMed: 20593496]

Wang J. Preclinical and clinical research on inflammation after intracerebral hemorrhage. Prog Neurobiol. 2010; 92:463–477. [PubMed: 20713126]

Whittle BJ, Varga C. New light on the anti-colitic actions of therapeutic aminosalicylates: the role of heme oxygenase. Pharmacol Rep. 2010; 62:548–556. [PubMed: 20631420]

Winder BS, Salmon AG, Marty MA. Inhalation of an essential metal: development of reference exposure levels for manganese. Regul Toxicol Pharmacol. 2010; 57:195–199. [PubMed: 20176068]

Zhang P, Hatter A, Liu B. Manganese chloride stimulates rat microglia to release hydrogen peroxide. Toxicol Lett. 2007; 173:88–100. [PubMed: 17669604]

Zhao Z, Chen Y, Wang J, Sternberg P, Freeman ML, Grossniklaus HE, et al. Age-related retinopathy in NRF2-deficient mice. PloS one. 2011; 6:e19456. [PubMed: 21559389]

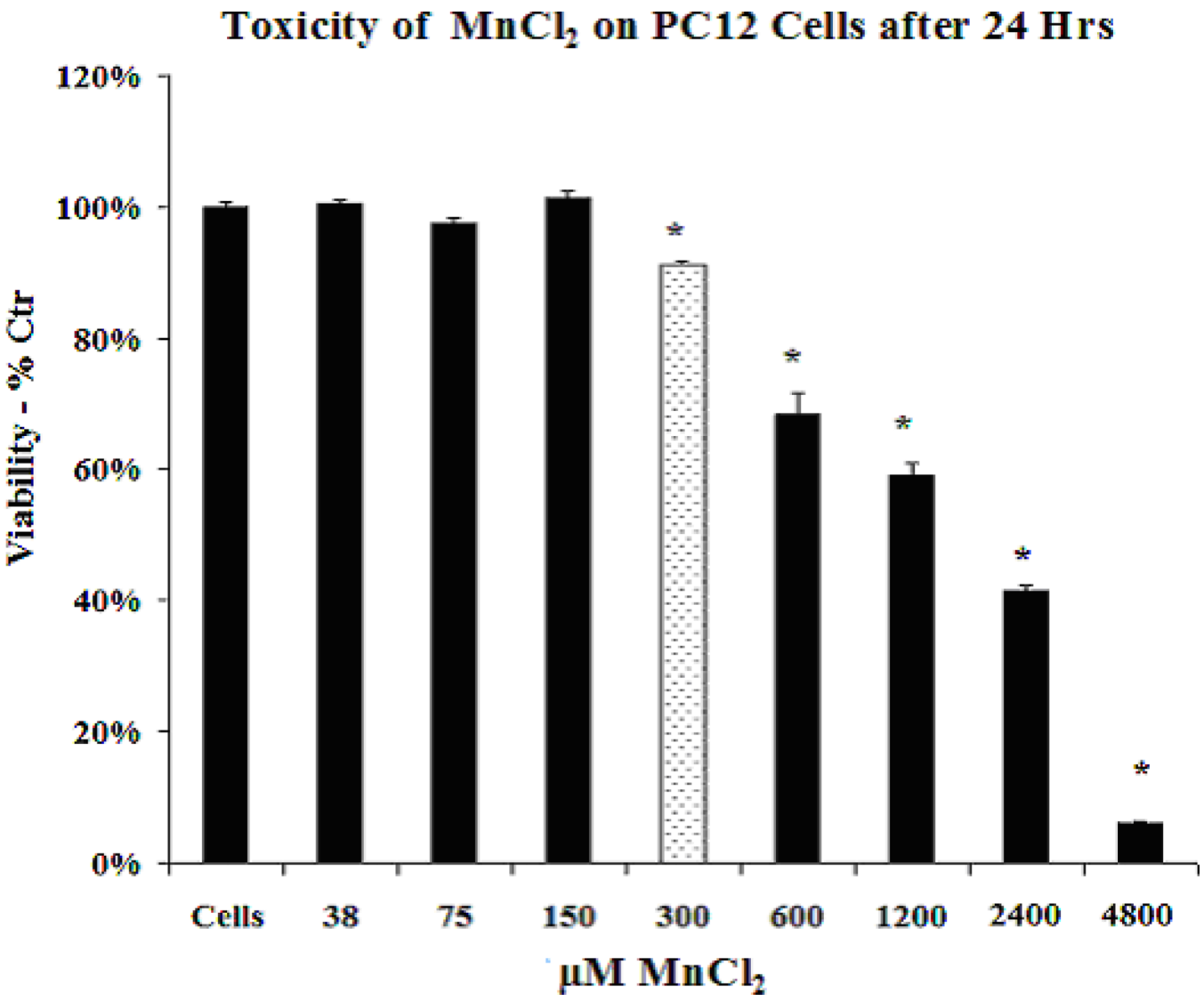

Figure 1.

Toxicity of $MnCl_2$ on PC12 Cells after 24 Hrs incubation. The data represent cell viability as % Control and are presented as the Mean ± S.E.M , n=4. Differences from the control were analyzed using a one-way ANOVA followed by a Tukey post hoc test. * p<.05.

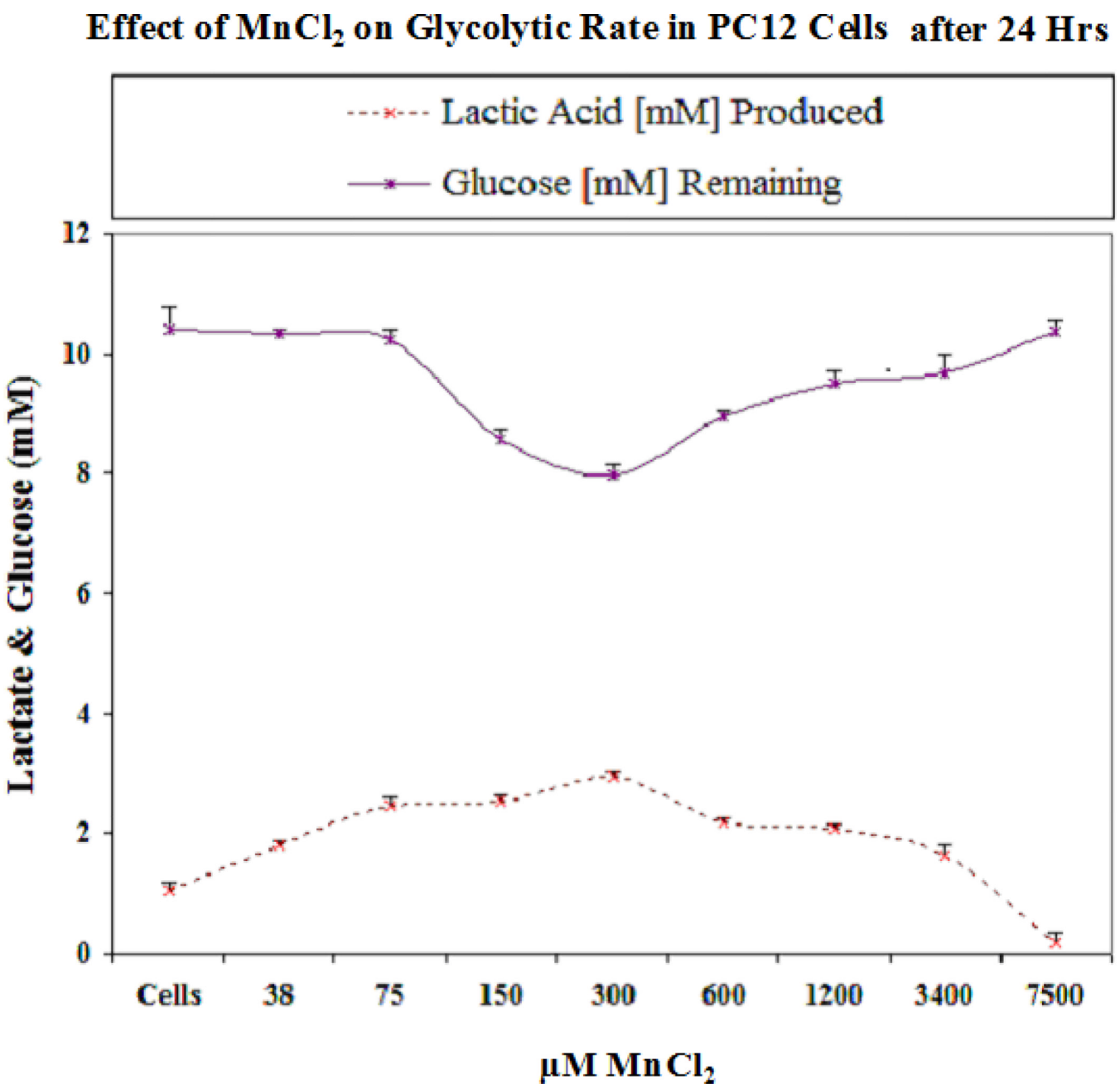

Figure 2.

Change of glucose consumption/ lactic acid production profile in $MnCl_2$ treated PC12 cells at 24 Hrs incubation. The data represent concentration of glucose mM or lactate mM in the supernatant and are presented as the Mean ± S.E.M , n=4.

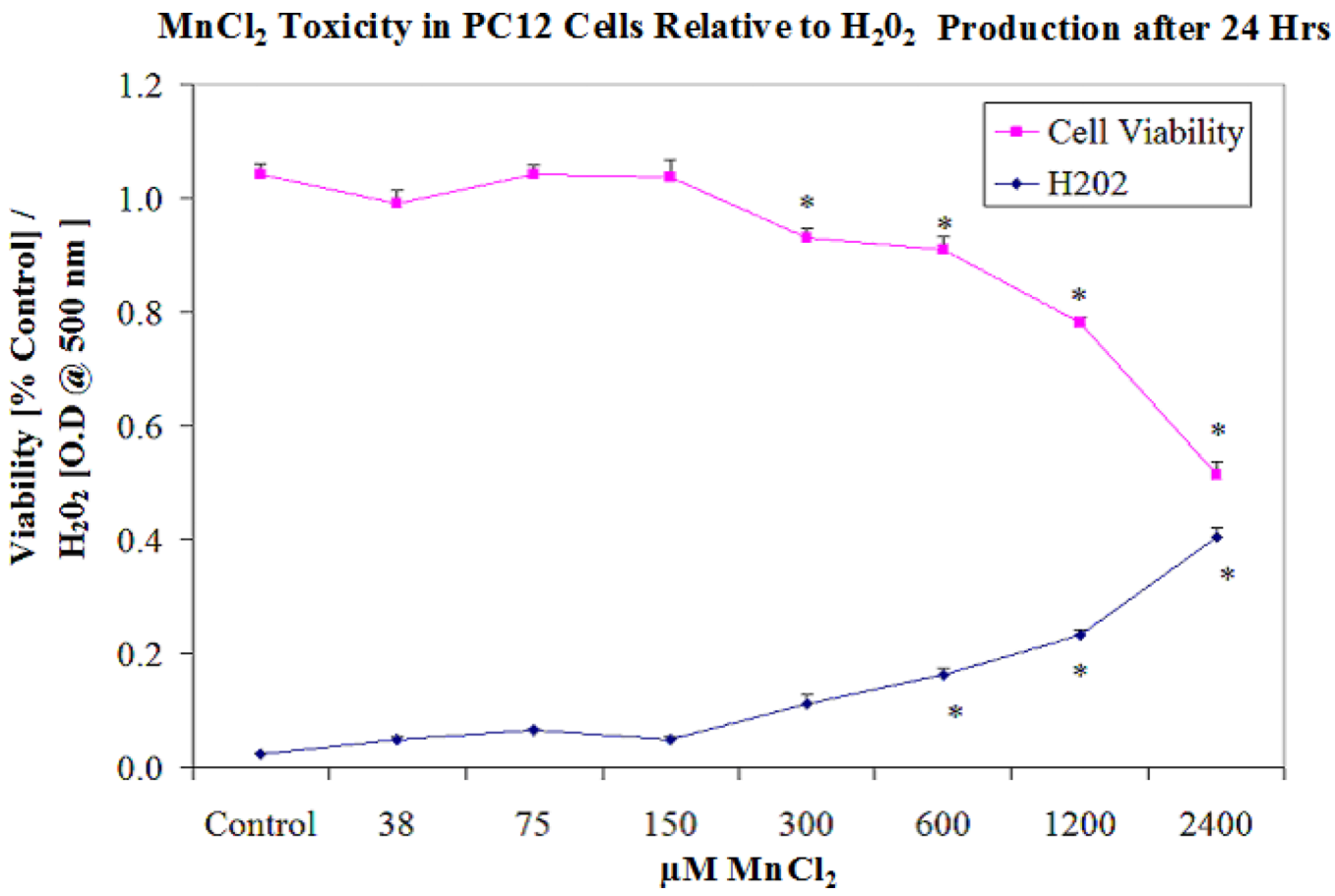

Figure 3.

MnCl2 Toxicity in PC12 cells relative to H_20_2 production after 24 Hr. The data represent cell viability as [% Control] and H_20_2 [O.D. 500 *nm*] produced and are presented as the Mean ± S.E.M , n=4. Differences from the control were analyzed using a one-way ANOVA followed by a Tukey post hoc test. * p<.05.

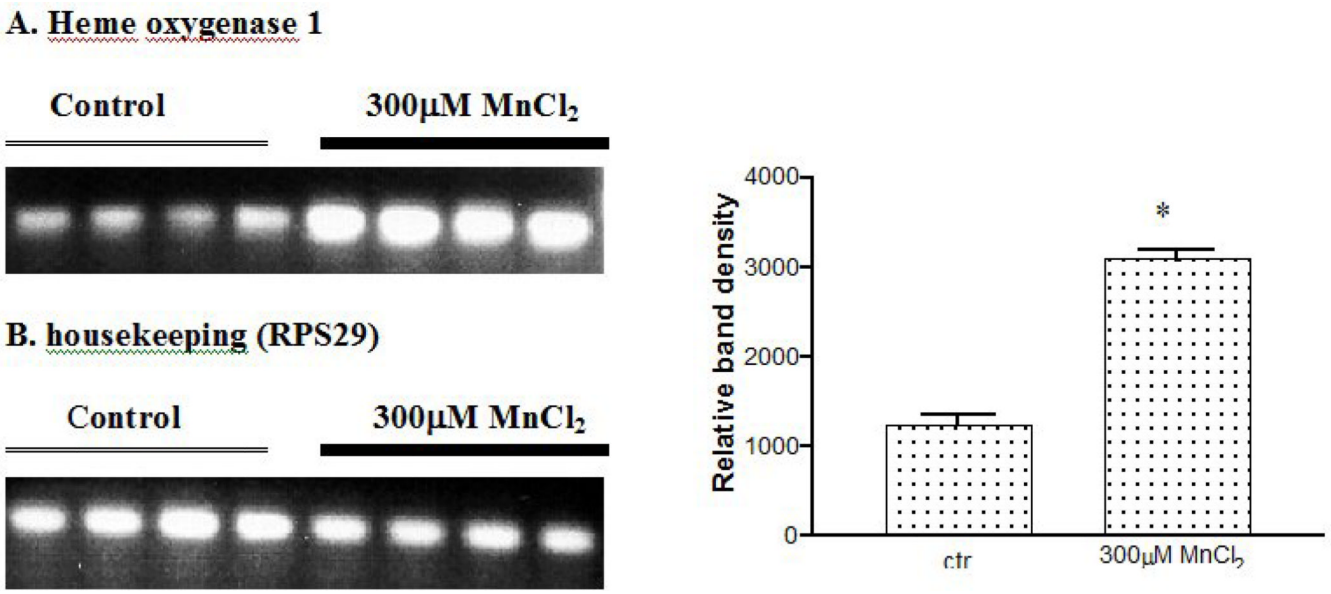

Figure 4.

HO-1 expression in $MnCl_2$ treated PC12 cells after 24 Hrs incubation. Verification of altered gene expression of array was performed by RT-PCR. HO-1 band intensities were measured using Molecular Dynamics 300 Series Computing Densitometer (4A), normalized against corresponding RPS29 housekeeping bands (4B). The data represent the Mean ± S.E.M , n=3 and difference from the control was analyzed using a students t-test. * $p<.05$.

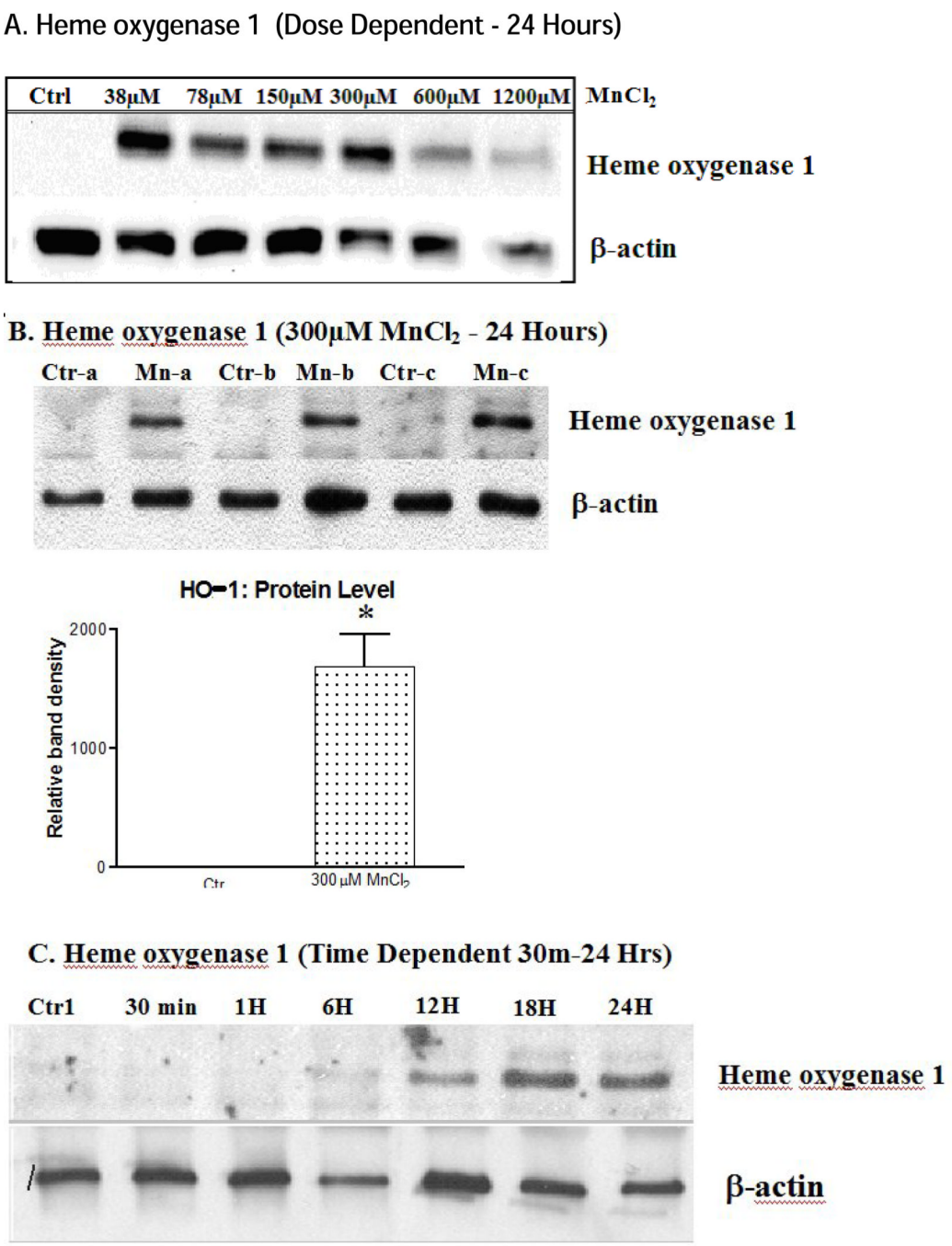

Figure 5.

HO-1 protein expression in $MnCl_2$ treated PC12 cells. Verification of altered protein expression was performed by western blot analysis, relative to β-actin loading controls. HOX-1 expression was monitored by dose (5A) , confirmed at 300µM $MnCl_2$ (5B) where the data represent band intensities and are presented as the mean ± S.E.M , n=3. The difference from the control was analyzed using a students t-test. * $p<.05$. Time dependent [30 m – 24 Hrs] HOX-1 induction using 300µM $MnCl_2$ was also assessed (5C).

Table 1

Differential gene expression profiles in PC12 cells treated with 300μM $MnCl_2$ vs untreated Controls for 24 Hrs.

	Gene Description		% Change	p-value
Oxidative Stress	*heme oxygenase (decycling) 1*	▲	**7.70**	0.001
	dithiolethione-inducible gene-1 (DIG-1).	▲	**6.19**	0.01
	acid phosphatase 5, tartrate resistant	▲	**4.72**	0.003
	arsenite inducible RNA associated protein (Airap)	▲	**5.61**	0.01
	Thioredoxin reductase 1	▲	**3.15**	0.04
	Biliverdin reductase A	▲	**1.37**	0.03
	Gene Description		**% Change**	**p-value**
Glycolysis	*Mouse hypoxia induced gene 2 (Hig2)*	▲	**4.83**	0.006
	Aldo-keto reductase family 1, member B1 (aldose reductase)	▲	**3.62**	0.007
	Enolase 2, gamma, neuronal	▲	**2.95**	0.003
	Aldolase A, fructose-bisphosphate	▲	**2.27**	0.000
Mitochondrial	*Glutaryl-Coenzyme A dehydrogenase mitochondrial transcript variant 1*	▼	**1.88**	0.000.
	ATP synthase, H+ transporting, mitochondrial F1, gamma polypeptide 1	▼	**1.59**	0.003
	Succinate dehydrogenase complex, subunit A, flavoprotein (Fp)	▼	**1.53**	0.040

▲upregulated genes

▼down regulated genes